

ND-A184 231

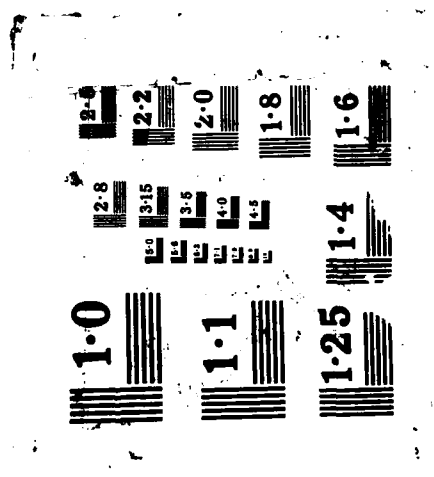
FAR-INFRARED SPECTRA OF LITHIUM DEPOSITED ON A GOLD
ELECTRODE INTERPRETA (U) OAKLAND UNIV ROCHESTER MICH
DEPT OF CHEMISTRY M W SEVERSON ET AL JUL 87 TR-28
N00014-77-C-0239 F/G 7/4

1/1

UNCLASSIFIED

NL





UNCLASSIFIED
SECURITY CLASSIFICATION

DTIC FILE COPY

12

AD-A184 231

ENTATION PAGE

1a. REPORT SECURITY

Unclassified

1b. RESTRICTIVE MARKINGS

none

2a. SECURITY CLASSIFICATION AUTHORITY

3. DISTRIBUTION/AVAILABILITY OF REPORT

2b. DECLASSIFICATION/DOWNGRADING SCHEDULE

Unrestricted

4. PERFORMING ORGANIZATION REPORT NUMBER(S)

Technical Report No. 28

5. MONITORING ORGANIZATION REPORT NUMBER(S)

ONR

6a. NAME OF PERFORMING ORGANIZATION

Oakland University

6b. OFFICE SYMBOL
(if applicable)

7a. NAME OF MONITORING ORGANIZATION

Office of Naval Research

6c. ADDRESS (City, State, and ZIP Code)

Department of Chemistry
Rochester, Michigan 48063

7b. ADDRESS (City, State, and ZIP Code)

800 N Quincy St.
Arlington, VA 22217

8a. NAME OF FUNDING/SPONSORING
ORGANIZATION

Office of Naval Research

8b. OFFICE SYMBOL
(if applicable)

9. PROCUREMENT INSTRUMENT IDENTIFICATION NUMBER

8c. ADDRESS (City, State, and ZIP Code)

800 N. Quincy St.,
Arlington, VA 22217

10. SOURCE OF FUNDING NUMBERS

PROGRAM
ELEMENT NO.

PROJECT
NO.

N00014-
77-C-0239

TASK
NO.

4133006

WORK UNIT
ACCESSION NO.

11. TITLE (Include Security Classification)

Far-infrared spectrum of lithium deposited on a gold electrode: interpretation using
a cluster model

12. PERSONAL AUTHOR(S)

M. W. Severson, P. P. Schmidt, S. Pons, J. Li, and J. J. Smith

13a. TYPE OF REPORT

Technical

13b. TIME COVERED

FROM TO

14. DATE OF REPORT (Year, Month, Day)

August 5, 1987

15. PAGE COUNT

17

16. SUPPLEMENTARY NOTATION

Physical Review, in press

17. COSATI CODES

FIELD

GROUP

SUB-GROUP

18. SUBJECT TERMS (Continue on reverse if necessary and identify by block number)

Solid/surface infrared spectroscopy

19. ABSTRACT (Continue on reverse if necessary and identify by block number)

A cluster model for the calculation of surface atom vibrations is described. The model assumes central forces between all the atoms of the cluster. Using a Morse function for the potential energy, the model is used to interpret the recently reported far-infrared spectrum of lithium deposited on a gold electrode.

20. DISTRIBUTION/AVAILABILITY OF ABSTRACT

☐ UNCLASSIFIED/UNLIMITED ☐ SAME AS RPT. ☐ DTIC USERS

21. ABSTRACT SECURITY CLASSIFICATION

22a. NAME OF RESPONSIBLE INDIVIDUAL

22b. TELEPHONE (Include Area Code)

22c. OFFICE SYMBOL

OFFICE OF NAVAL RESEARCH

Contract No. N00014-77-C-0239

R&T Code 4133006

Technical Report No. 28

Far-Infrared spectra of lithium deposited on a gold electrode;
interpretation using a cluster model

by

M. W. Severson, P. P. Schmidt, S. Pons, J. Li, and J. J. Smith

Prepared for Publication in
Physical Review

Oakland University
Department of Chemistry
Rochester, Michigan 48063

July 1987

Reproduction in whole or in part is permitted for
any purpose of the United States Government

Approved for Public Release; Distribution Unlimited

Far-infrared Spectrum of Lithium Deposited on a Gold Electrode:

Interpretation Using a Cluster Model

by

Mark W. Severson^a, Stanley Pons^b, P. P. Schmidt^a,

Jianguo Li^b, and J. J. Smith^c

^aDepartment of Chemistry

Oakland University

Rochester, Michigan 48063

^bDepartment of Chemistry

University of Utah

Salt Lake City, Utah 84112

^cPhysics Department

Naval Weapons Center

China Lake, California 93555



Accession For	
NTIS GRA&I	<input checked="" type="checkbox"/>
DTIC TAB	<input type="checkbox"/>
Unannounced	<input type="checkbox"/>
Justification	
By	
Distribution /	
Avail and/or Codes	
1 Avail and/or Special	
Dit	
A-1	

Abstract

A cluster model for the calculation of surface atom vibrations is described. The model assumes central forces between all the atoms of the cluster. Using a Morse function for the potential energy, the model is used to interpret the recently reported far-infrared spectrum of lithium deposited on a gold electrode.

Introduction

Recently, Li, Pons, and Smith¹ have reported far-infrared spectra of a gold electrode surface in an acetonitrile solution of lithium perchlorate. At electrode potentials at which lithium is not deposited on the gold surface, they observed a number of bands between 130 and 170 cm^{-1} which they assigned to vibrations of the gold atoms in the surface layer. These spectra are shown in Fig. 1. At potentials at which the underpotential deposition of lithium occurs, these bands disappeared, and a band at 440 cm^{-1} grew in, as shown in Fig. 2b. At potentials at which the bulk deposition of lithium begins, a band at 400 cm^{-1} appears, as shown in Fig. 2c. Experiments using the ^6Li isotope showed that both the band at 440 cm^{-1} and that at 400 cm^{-1} are due to vibrations of lithium atoms; the bands at about 600 cm^{-1} did not show an isotope shift, and may be assigned to vibrations of the perchlorate anion.

In this paper we describe a cluster model for the calculation of the vibrations of a solid surface in which each atom of the cluster is assumed to interact with all of the other atoms of the cluster through central forces. We report results calculated using this model for the Au(111) surface, and for this surface with layers of deposited lithium. We use this model to interpret the observed infrared spectra for lithium deposition on gold.

Cluster Model for Metal Surface Vibrations

Calculation of surface metal atom and adsorbate vibrations using cluster models have been successful in describing the dynamics of these systems.² These

previous calculations have used nearest-neighbor force constants. Here we describe the use of explicit functional forms for the potential energy operating between the atoms of the cluster, and show a convenient way in which more than nearest-neighbor terms may be included. The model which we have used for the metal surface is a cluster of 125 atoms arranged in five layers of a face-centered cubic (111) geometry. We assumed that each metal atom interacts with all of the other atoms in the cluster through a Morse potential function

$$V_M(r) = D \exp[a(R_0 - R)]\{\exp[a(R_0 - R)] - 2\} \quad (1)$$

Since we assumed only central forces, we used a symmetry-adaptable Taylor series which has been reported previously³ to obtain the force constants in cartesian displacement coordinates. When considering the interactions of a given atom of the cluster with other atoms, there are two types of force constants which arise. The first type is a single species force constant; for a species A which is surrounded by species B...Z, one finds force constants of the form

$$k_{ii}^A = \sum_{I=B}^Z k_{ii}^{AI} \quad (2)$$

for the cartesian diagonal terms and

$$k_{ij}^A = \sum_{I=B}^Z k_{ij}^{AI} \quad (3)$$

for the single center, cartesian non-diagonal contributions. In these equations,

$$k_{11}^{IJ} = \frac{1}{3} \{ I_{20}(R) + (2X_1^2 - X_j^2 - X_k^2) I_{22}(R)/R^2 \} \quad (4)$$

and

$$k_{1j}^{IJ} = X_1 X_j I_{22}(R)/R^2 \quad (5)$$

where $R = R_I - R_j$, the lower case indices i and j label the cartesian coordinates, and the upper case indices I and J label the atoms. The second type is a species non-diagonal force constant; there is only one of these for each distinct pair of atoms, and one finds

$$k_{11}^{AB} = \frac{1}{3} \{ I_{20}(R) + (2X_{ABi}^2 - X_{ABj}^2 - X_{ABk}^2) I_{22}(R)/R^2 \} \quad (6)$$

for the species non-diagonal, cartesian-diagonal terms and

$$k_{1j}^{AB} = X_{ABi} X_{ABj} I_{22}(R)/R^2 \quad (7)$$

for the species non-diagonal, cartesian non-diagonal terms. The terms I_{20} and I_{22} which appear in equations (4) through (7) are

$$I_{20}(R) = \frac{d^2 V}{dR^2} + \frac{2}{R} \frac{dV}{dR} \quad (8)$$

and

$$I_{22}(R) = \frac{d^2 V}{dR^2} - \frac{1}{R} \frac{dV}{dR} \quad (9)$$

In order to simulate a semi-infinite crystal, we imposed periodic boundary conditions in the directions parallel to the surface in the following way. When calculating the force constants of equations (2) through (7), the coordinates of

all the atoms in the cluster were shifted such that atom A was at the center of its layer; this was done for each atom of the cluster in turn. r_0 in the Morse function, equation (1), was chosen to give zero force on the central atom of the cluster when the internuclear distance was that of gold. The position of the top layer was then adjusted to give zero force on these atoms as well. Since the parameters we chose resulted in the Morse function being fairly short-ranged, this surface relaxation was rather small, about 0.005 Å. In this cluster model, we consider interactions between all atoms, not just nearest neighbors; as a result, the first derivatives in I_{20} and I_{22} , equations (8) and (9), will not, in general, vanish. Note that there are two surfaces in this model; we tried eliminating the bottom surface by including rigid layers below the bottom layer, but we found that this made insignificant differences in the calculated results. Spectral density functions² were calculated, assuming a Lorentzian lineshape:

$$\rho_{\alpha\beta}(ll';\omega,\gamma) = e_{\alpha}^s(l)e_{\beta}^s(l')\{\gamma/[(\omega - \omega_s)^2 + \gamma^2]\}$$

where α, β label the cartesian coordinates, l and l' label the atoms, s labels the normal mode, $e_{\alpha}^s(l)$ are the eigenvectors obtained from diagonalization of the cartesian force constant matrix, γ is the width parameter, and ω is the frequency. For all of the calculations reported here, we used $\gamma = 7 \text{ cm}^{-1}$. This quantity, together with a model for the change in dipole moment with a vibration, allows calculation of the expected infrared spectrum. We assumed that the change in dipole moment is due to oscillations of the atoms in the top layer only; in this case, the infrared spectrum is directly proportional to the spectral density for the zero-wavevector mode, in which all the atoms in the top layer vibrate in phase.

Results

In order to test the cluster model, we calculated spectral density functions for motion of a single gold atom in the (111) surface layer in the direction parallel and perpendicular to the surface, since a calculation of these quantities using the continued fraction method has been reported.⁴ The results are shown in Fig. 3, and these are quite similar to the continued fraction results of ref. 4. In Fig. 4a we show the calculated zero-wavevector spectral density for the Au(111) surface for two different values of the Morse energy D between the first and second layer. For the first of these we used the value of D appropriate to bulk gold, which was the same as that used to generate the spectral densities of Fig. 1. In the second, we increased the value of D between the first and second layers. Li et. al. used the subtractively normalized interfacial Fourier transform infrared spectroscopy (SNIFTIRS) technique to obtain the far-infrared spectra of the gold electrode; this technique gives the difference of the spectra at two different electrode potentials. We assumed that the effect of changing the electrode potential was to change the value of D . The resulting difference, shown in Fig. 4b, is qualitatively similar to the infrared spectra of Li et. al.¹, Fig. 1.

Next we simulated the situation in which a monolayer of lithium has been deposited on the Au(111) surface by replacing the top layer of gold atoms with lithium atoms. This amounted to changing the masses only; we used the same potential function parameters and atomic positions. The result of this calculation, Fig. 5, shows a single band at about 440 cm^{-1} , which is just what is observed experimentally, cf. Fig. 2.

We simulated the bulk deposition of lithium with a model in which the top two layers of the cluster were lithium atoms. Using the same parameters as for the calculation of Fig. 5, we obtained two bands, one at about 260 cm^{-1} and the other at about 605 cm^{-1} . The lower wavenumber band corresponds to the mode in which the two lithium layers are moving in the same direction, and the higher wavenumber band to that in which the two layers are moving in opposite directions. The calculated intensity of the lower wavenumber band is about twice that of the higher wavenumber band. This spectrum is shown as curve (a) of Fig. 8. Experimentally, a single band at 400 cm^{-1} is observed at potentials at which the bulk deposition of lithium begins, cf. Fig. 2. We considered two ways in which the calculation could give a band at 400 cm^{-1} , matching experiment. First we assumed that the 400 cm^{-1} band was due to the two lithium layers moving in opposite directions. We left the interaction energy for Au-Li unchanged, and reduced the Li-Li interaction energy. The results of this calculation are shown in Fig. 6, from which it can be seen that as the Li-Li energy term is reduced enough that the band approaches 400 cm^{-1} , its intensity, relative to the lower wavenumber band, becomes very small. Next we did a similar calculation, with the Au-Li interaction energy decreased by a factor of ten. The results of this calculation, plotted in Fig. 7, show that with the proper choice of parameters there is a band with appreciable intensity near 400 cm^{-1} , and a second band at about 100 cm^{-1} . We also investigated a range of other choices for the interaction energies, and found that for this model, if the 400 cm^{-1} band is due to the motion of the two lithium layers in opposite directions, there is always a second band between 100 and 300 cm^{-1} of equal or greater intensity. No such band was observed in the infrared spectrum under these conditions.

Next we considered the possibility that the 400 cm^{-1} band is due to the

motion of the two Li layers in the same direction. To do this, we kept the Li-Li interaction energy fixed at the value used for Figure 5, and increased the Au-Li interaction energy. The results of this calculation are shown in Fig. 8. From this we see that as the Au-Li energy is increased, the lower wavenumber band approaches 400 cm^{-1} , and the higher wavenumber band is shifted to much higher values. As the lower wavenumber band approaches 400 cm^{-1} , its intensity relative to the higher wavenumber band increases dramatically; in curve (e) of Fig. 8, the relative intensities are about 20:1. This matches the experimental result, if we assume that the higher wavenumber band is of such low intensity that it is not observed experimentally.

Discussion

The cluster model which we have used seems to give a good description of the vibrations of surface atoms in Au(111), as can be seen by comparing the parallel and perpendicular spectral density functions which we obtain, shown in Figure 3, with those obtained using the continued fraction method.⁴ An appealing aspect of the model we have described is that it can account for surface relaxation in a natural way. In simulating the SNIFTIRS spectrum of the clean gold electrode, we assumed that the effect of changing the electrode potential was to change the energy term in the Morse potential, but any small change in the potential energy function would give similar results. Since our calculation was for the Au(111) surface, while the experimental results were obtained for a polycrystalline sample, we have not attempted to match the experimental results exactly; it is enough to show that the calculation predicts bands in the same region of the spectrum in which they are observed experimentally.

For the calculations with one and two layers of lithium on the gold surface, we obtained excellent agreement with the experimental results. Since we did not know the actual geometry appropriate for the deposited lithium, we assumed it to be identical to gold; the actual geometry is undoubtedly different. We have also neglected three-center and higher order terms in the potential energy function. Thus, the potential energy parameters with which we matched the experimental results should be regarded as effective parameters. It is possible that use of the actual geometry would give qualitatively different results from those we have obtained. However, lacking that information, we believe that our assignment of the band at 400 cm^{-1} to the motion of two layers of lithium moving in the same direction is a reasonable one.

References

1. J. Li, S. Pons, J. J. Smith, Langmuir **2**, 297, (1986).
2. See for example, K. G. Lloyd, J. C. Hemminger, J. Chem. Phys. **82**, 3858, (1985); J. C. Ariyasu, D. L. Mills, K. G. Lloyd, J. C. Hemminger, Phys. Rev. B. **30**, 507, (1984).
3. M. W. Severson, P. P. Schmidt, J. M. McKinley, J. Chem. Phys. **86**, 5392, (1987).
4. G. Treglia, M.-C. Desjonquieres, J. Physique **46**, 987, (1985).

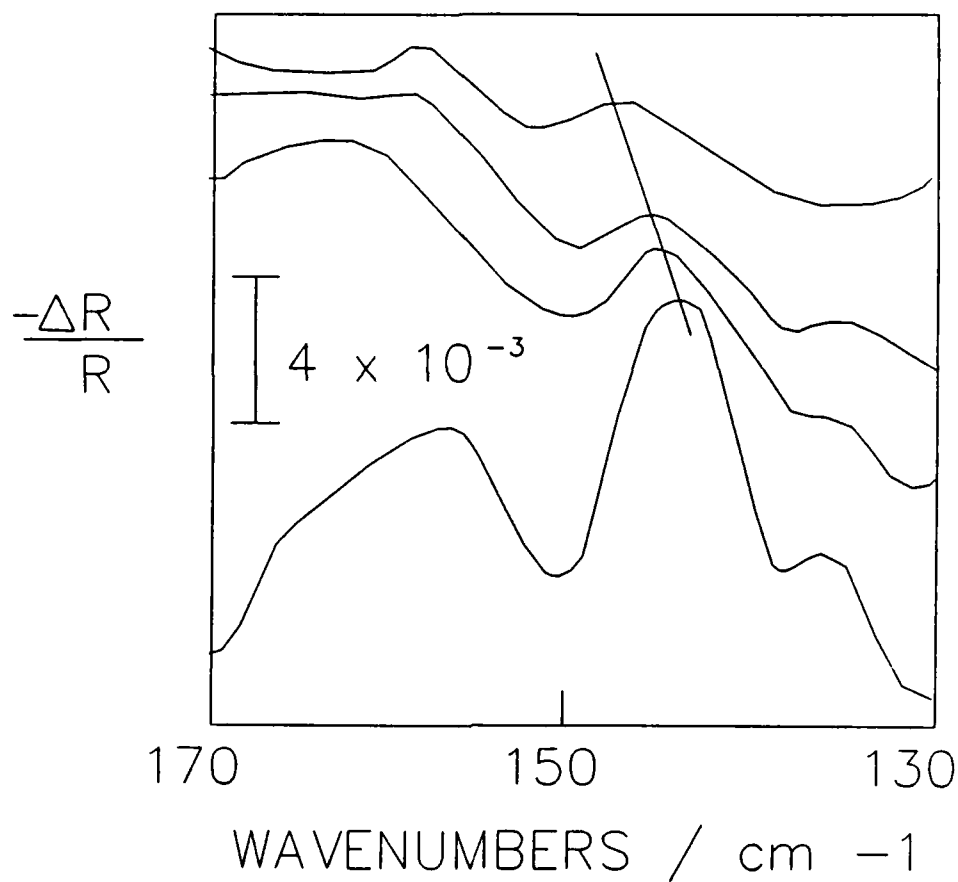


Figure 1. Far-infrared SNIFTIRS spectra of the gold electrode surface as a function of electrode potential. The curves represent potentials of (top to bottom) -1.70, -1.90, -2.60, and -2.90 V, with reference potential -1.50 V. Potentials are relative to the reference electrode, which was Ag/Ag⁺, 0.01 M AgNO₃ in acetonitrile.

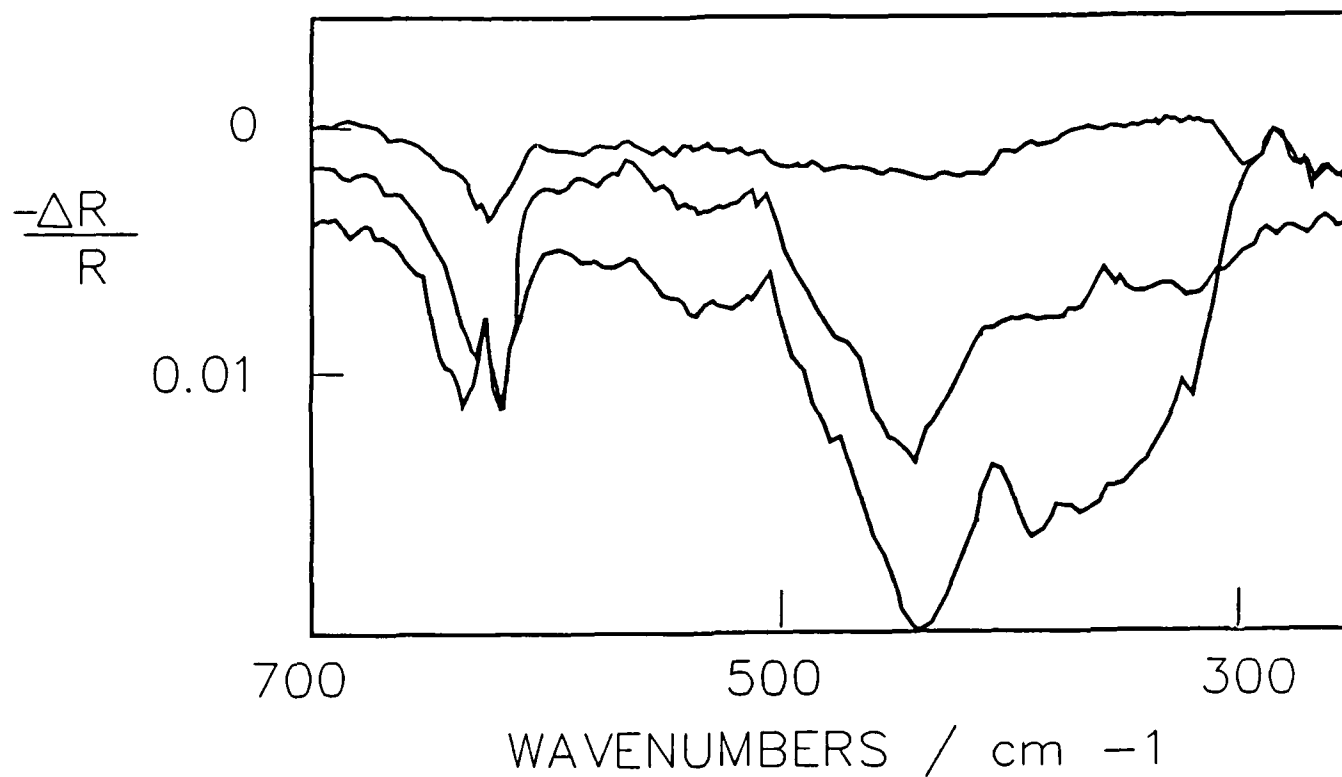


Figure 2. Far-infrared SNIFTIRS spectra of lithium on the gold electrode surface as a function of electrode potential. The curves represent potentials of (top to bottom) -1.70, -2.90, and -3.00 V, with reference potential -1.50 V.

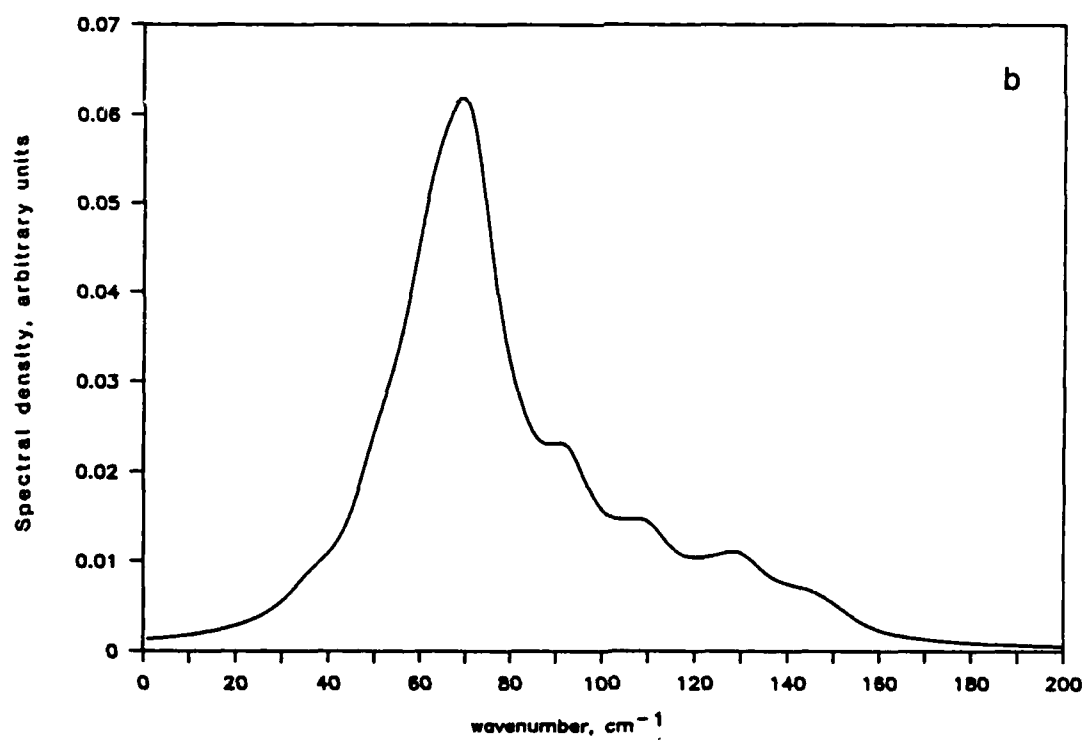
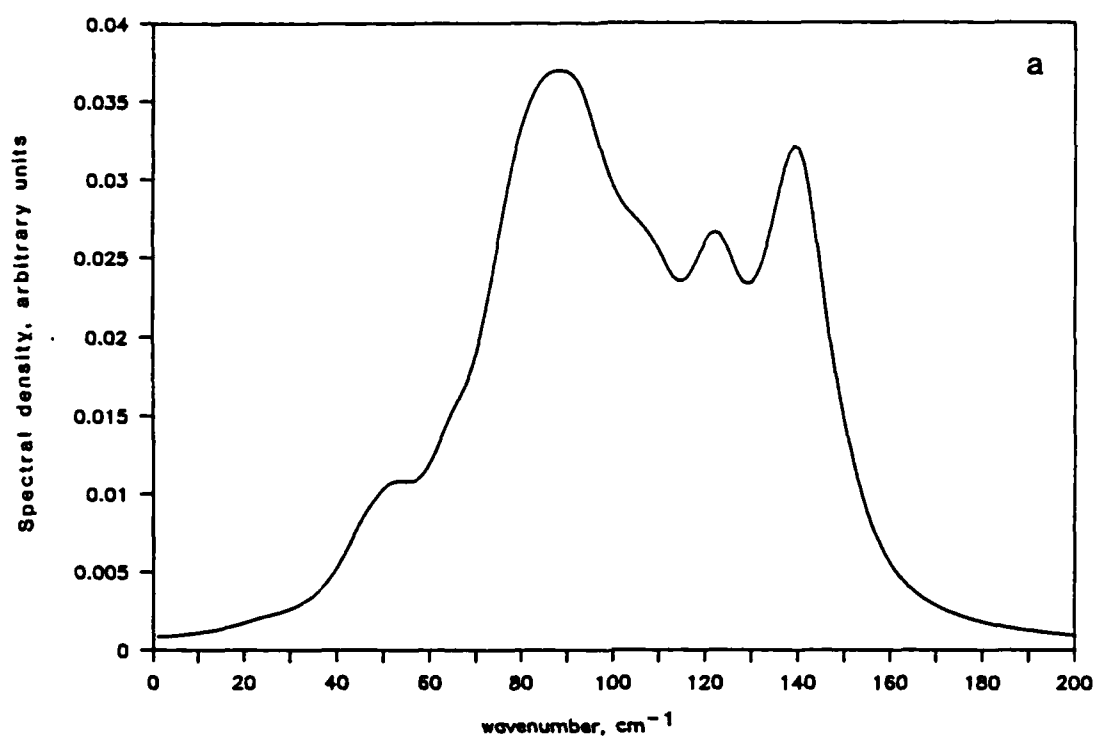


Figure 3. Spectral density functions for motion of a single atom in the Au(111) surface. Parameters in Morse function: $D = 0.0197$ aJ, $a = 3 \text{ \AA}^{-1}$, $r_0 = 2.888 \text{ \AA}$. a. Parallel spectral density. b. Perpendicular spectral density.

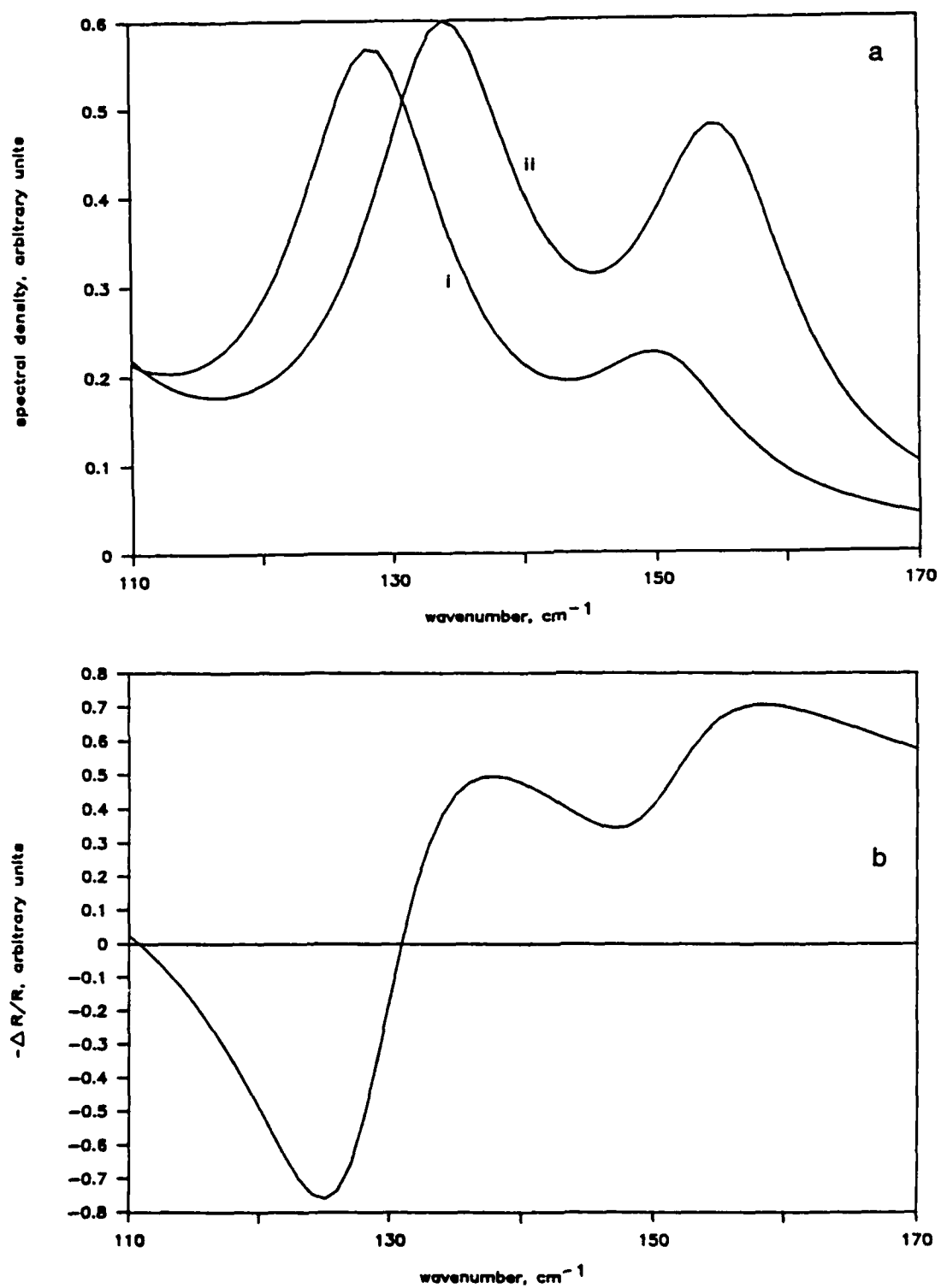


Figure 4. Zero wavevector spectral densities and simulated SNIFTIRS spectrum for Au(111). a.) curve I calculated with $D = 0.0197 \text{ aJ}$, $a = 3 \text{ \AA}^{-1}$, $r_0 = 2.888 \text{ \AA}$. curve II calculated with $D = 0.025 \text{ aJ}$, $a = 3 \text{ \AA}^{-1}$, $r_0 = 2.888 \text{ \AA}$. b.) Simulated SNIFTIRS spectrum: difference between curve I and curve II of Fig. 2a.

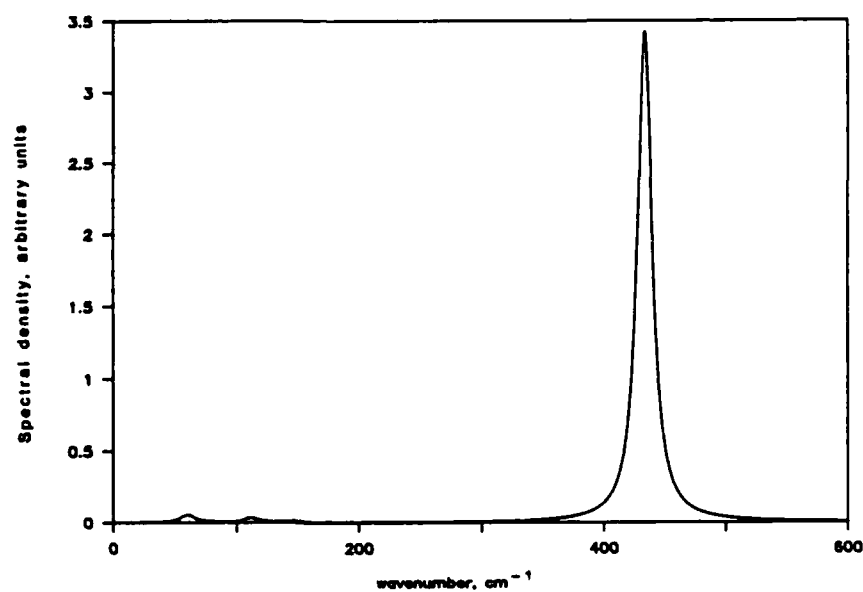


Figure 5. Zero wavevector mode for one layer of lithium on Au(111). The parameters used are the same as in Figure 3.

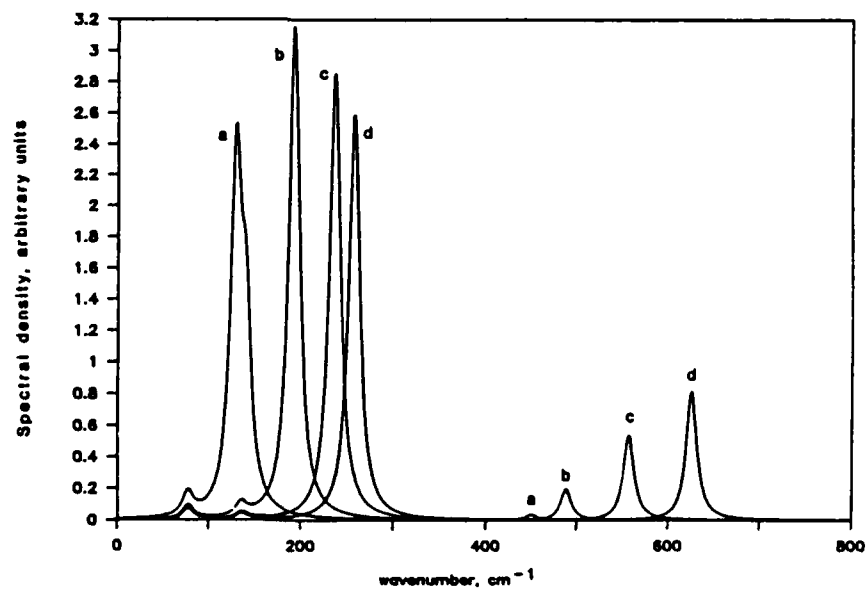


Figure 6. Zero wavevector mode for two layers of lithium on Au(111); effect of varying the Li-Li interaction energy using parameters for the Au-Au and Au-Li interaction of $D = 0.0197$ aJ, $a = 3 \text{ \AA}^{-1}$, $r_0 = 2.888 \text{ \AA}$. For the Li-Li interaction $a = 3 \text{ \AA}^{-1}$, $r_0 = 2.888 \text{ \AA}$, and a.) $D(\text{Li-Li}) = 0.002$ aJ; b.) $D(\text{Li-Li}) = 0.005$ aJ; c.) $D(\text{Li-Li}) = 0.01$ aJ d.) $D(\text{Li-Li}) = 0.015$ aJ.

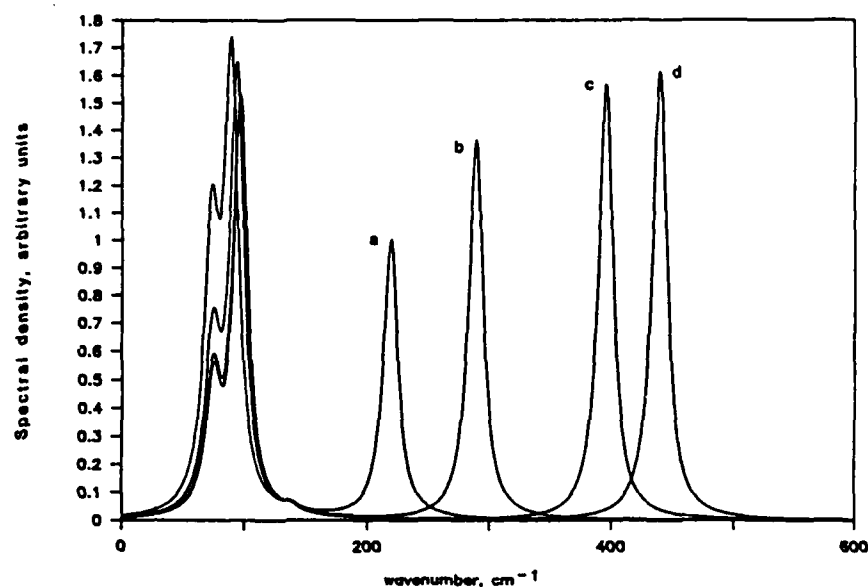


Figure 7. Zero wavevector mode for two layers of lithium on Au(111); effect of varying the Li-Li interaction energy using parameters for the Au-Au interaction of $D = 0.0197$ and for the Au-Li interaction of $D = 0.002$ aJ; for both, $a = 3 \text{ \AA}^{-1}$, $r_0 = 2.888 \text{ \AA}$. For the Li-Li interaction $a = 3 \text{ \AA}^{-1}$, $r_0 = 2.888 \text{ \AA}$, and
a.) $D(\text{Li-Li}) = 0.002$ aJ; b.) $D(\text{Li-Li}) = 0.004$ aJ; c.) $D(\text{Li-Li}) = 0.008$ aJ
d.) $D(\text{Li-Li}) = 0.01$ aJ.

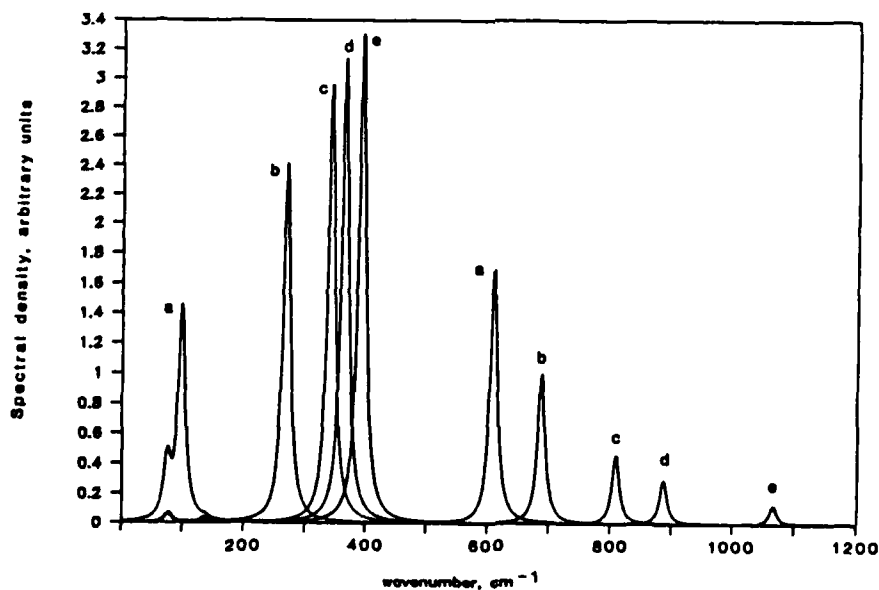


Figure 8. Zero wavevector mode for two layers of lithium on Au(111); effect of varying the Au-Li interaction energy using parameters for the Au-Au and Li-Li interaction of $D = 0.0197$ aJ, $a = 3 \text{ \AA}^{-1}$, $r_0 = 2.888 \text{ \AA}$. For the Au-Li interaction $a = 3 \text{ \AA}^{-1}$, $r_0 = 2.888 \text{ \AA}$, and
a.) $D(\text{Au-Li}) = 0.002$ aJ; b.) $D(\text{Au-Li}) = 0.0197$ aJ;
c.) $D(\text{Au-Li}) = 0.044$ aJ; d.) $D(\text{Au-Li}) = 0.08$ aJ; e.) $D(\text{Au-Li}) = 0.01$ aJ.

END

10-87

DTIC